Rainy with a Chance of Sea Salt: Sourcing the Sulfur in Houston's Rainfall

Valentina Osorio

Senior Honors Thesis
Department of Earth, Environmental, and Planetary Sciences
Rice University, Houston, TX 77005
Spring 2024

Principle Investigator: Mark Torres, Ph.D.
Primary Mentor: William Larsen
Other mentors: Tao Sun, Ph.D. & Haolin Zhou

Abstract

As one of six criteria air pollutants monitored by the US Environmental Protection Agency, sulfur dioxide (SO_2) negatively affects human and environmental health. Upon entering the atmosphere, SO_2 is oxidized and dissolved in water as sulfuric acid (H_2SO_4); consequently sulfate (SO_4^{2-}) rains out and can act as a tracer for atmospheric processing of sulfur compounds. Precipitation data were taken in Houston and compared to the Attwater Prairie Chicken National Wildlife Refuge in order to compare sulfur sources in atmospheric deposition between urban and rural regions. Houston rain exhibits chemical signatures that are suggestive of seawater and dust influences on rain chemistry, but leaves uncertainty in attributions to these sources as well as others expected to be present around Houston. This project evaluates the degree to which solute and water isotope data can be used to source sulfate in rainfall both within the major city of Houston and outside of its large suburban area.

Acknowledgements
To Will, I couldn't ask for a better day-to-day mentor. You have helped me grow so much, and I aspire to engage in my research and to share science like you do.

To Mark, thank you for working with me to support my interests. I appreciate you being a funny and honest mentor who always makes time for questions.

To Tao, thank you for supporting my ambitions to work on sulfur isotopes. I learned so much from your work and am excited to continue working with you in the future.

To the Torres Lab, thank you for accepting me into your group and mentoring me for the past year. Thank you for the treats, laughs, and science.

To Helge and Juli, I appreciate your support throughout my time in the EEPS department. You both helped me learn field, coding, and writing skills that I cannot be more thankful for.

To Travis Cochran - Thank you for helping me access the KWGL roof.

To Old Man, you inspire me, and I hope I'm making you proud.

To Ximena, I appreciate your support ever since I was born. Thank you mucho for fostering my love of learning.

To Gabe and Pearl, Orgo budz will never die. I couldn't have gotten this far without you. I want good lava cake and bread.

To the Yu family, thank you for being my home at Rice. For bringing smiles to my face, laughter to my jokes, and so much love to my heart.

To my family and friends, thanks :)

Table of Contents

1. Introduction & Background

1.1 Motivation. Since 1970, sulfur dioxide (SO_2) and particulate matter (PM) have been considered "criteria pollutants" under the Environmental Protection Agency's (EPA's) Clean Air Act.[1] These two pollutants cause reduced visibility, exacerbate pre-existing cardiovascular and respiratory diseases, complications with pregnancies, and premature deaths.[2] Beyond the immediate health effects of SO_2, this gas is processed in the atmosphere to produce cascading effects within the Earth system such as the generation of sulfate (SO_4^{2-}) aerosols, which account for half of the global PM concentrations.[3] These aerosols are transported to the Earth's surface as acid rain which contributes to the acidification of natural bodies of water, resulting in habitat loss, biodiversity destruction, ecological imbalance, and effects on biogeochemical cycling.[4,5,6] According to the Intergovernmental Panel on Climate Change (IPCC), sulfate aerosols affect radiative forcing in magnitude just behind CO_2 by acting as cloud condensation nuclei (CCN) that facilitated cloud formation. As such, they modulate climate by increasing, or at least maintaining, Earth's albedo; however, their role in Earth systems is complex which results in big uncertainties in climate models.[7,8]

Just after the EPA's Clean Air Act, the National Atmospheric Deposition Program (NADP) established a precipitation monitoring network across the US starting in 1977 during the height of concerns over acid rain. Together these movements have resulted in an 87% decrease in anthropogenic emissions of SO_2 since 2002, mainly associated with the mitigation of sulfur compounds released in coal combustion.[1] Still, SO_2 and sulfate remain in considerable concentrations from other industrial processes such as fossil fuel burning and metal smelting. Growing concern over underreporting has resulted in continued research into emission inventories, including Houston,TX. This major US city presents a unique case study surrounded

by a variety of atmospheric sulfur inputs, such as petrochemical infrastructure, farmlands, and seawater from the Gulf of Mexico (discussed in *Section 1.2*). Despite the importance of this critical area, the NADP network's nearest sampling site is 60 miles west of the city at the Attwater Prairie Chicken National Wildlife Refuge.[9] The Gulf of Mexico has been a place of study for air quality and acid rain mitigation, exploring the interplay of a myriad of climate drivers using sulfate aerosols. Still, however, it remains that no study to date has investigated regional differences in rain chemistry as a metric for sourcing pollutants near the Houston Ship Channel.[10]

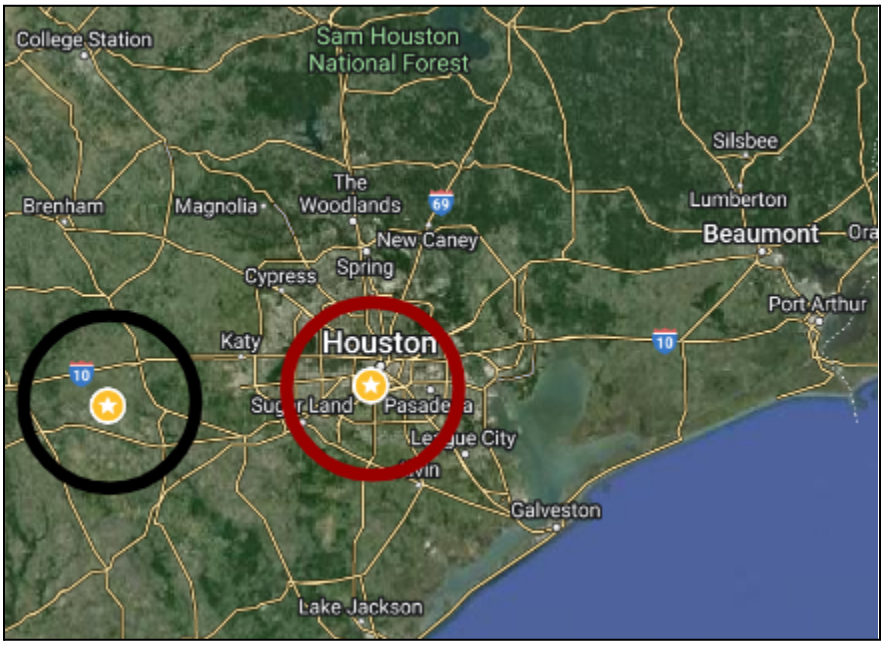

Figure 1: Map of Rice University (red) and NADP National Wildlife Refuge (black) rain collection sites.

1.2 Natural Sulfate Sources. Beyond anthropogenic influences, sulfur-containing gasses are emitted naturally from biogenic, oceanic, and volcanic sources. Active volcanoes release SO_2 as well as hydrogen sulfide (H_2S). H_2S is also released by soils, and dimethyl sulfide (DMS) is emitted from phytoplankton and soil biota.[8,11] The various sources of sulfur underscores the importance of parsing the cascading effects of human influence on the sulfur cycle. Revealing

the origins of atmospheric sulfate is vital to produce legislation that effectively targets non-natural emissions and informs the development of mitigation methods.

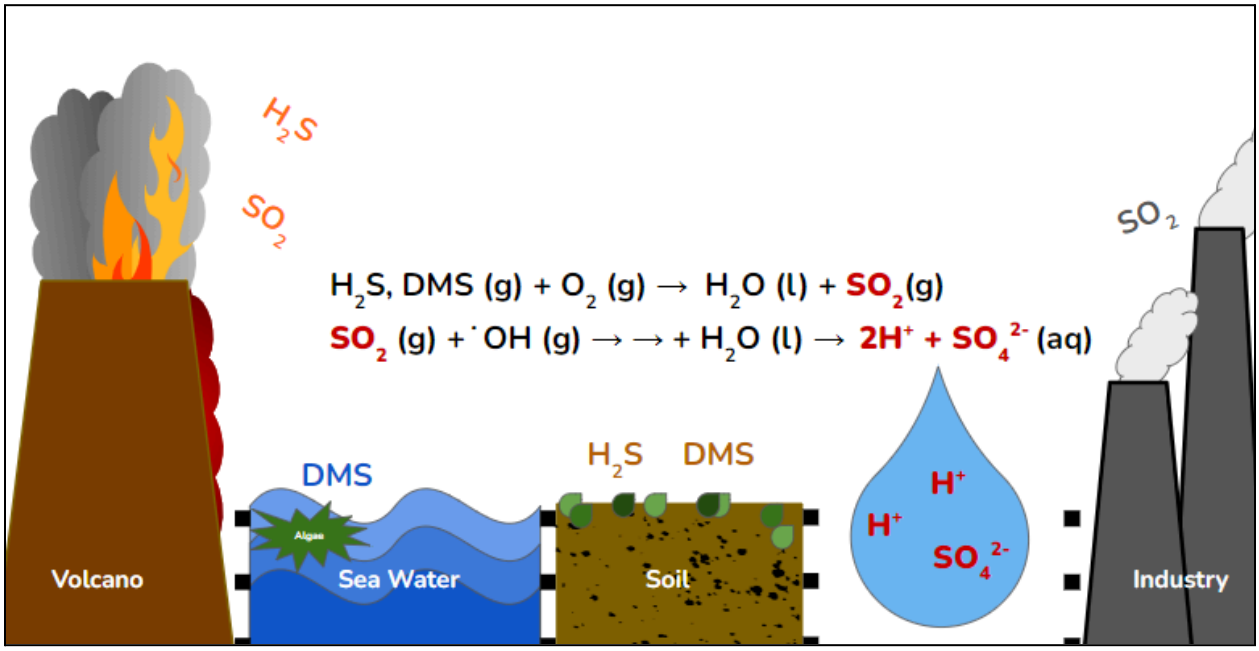

Figure 2: A simplified depiction of the sulfur cycle involving sulfur-containing gasses and solutions.

1.3 Chemical Pathways. Once sulfur-containing gasses enter the troposphere, their rates of oxidation into H_2SO_4 and sulfate aerosols depend on its surrounding conditions, such as temperature, clouds/fog, oxidant concentrations, and sunlight intensity. To date, discrete pathways from SO_2 to sulfate aerosols have been categorized into gas, aqueous, and aerosol phases. In the gas phase, the main oxidant is an OH radical, formed from photolytic cleavage. When OH radical concentrations are small, the role of Criegee biradicals, generated by nocturnal ozone (O_3) and alkene processing, has been thought to minimally contribute during the night. In the presence of an aqueous medium, SO_2 dissolves into hydrated SO_2, bisulfate ions, and sulfite ions. When dissolved in pure water, the species' concentrations are determined by an equilibrium process; however, in the presence of clouds and fog, sulfur species are found at higher

concentration than expected because of its formation of complexes with dissolved cations like Fe^{3+} and aldehyde species.[12]

Once sulfur compounds are dissolved into the bulk aqueous phase, they are oxidized to S (VI) in reactions with O_2, transition metal catalysts (Fe^{3+} and Mn^{2+}), ozone (O_3), peroxides (R_2O_2), nitrogen oxides (NO_x), and free radicals in clouds and fogs.[12] Sulfuric acid can also be formed when oxidation takes place on a solid surface, including mineral dust and carbon compounds. Active research is exploring these multiphase pathways that may be as important as aqueous oxidation.[13,14,15] Thus, dissolved ions in the rainwater record the sources and atmospheric processing of different pollutants, such as SO_2.

One study suggests that SO_2 oxidation in water, which is an important process affecting the acidity of rain, can be characterized by its reaction with atmospheric OH radicals below a pH of 4 and above 6. While this is thought to occur in a single step, the significance of the other oxidation pathways remains uncertain.[16] This hypothesis can be tested with current analytical chemistry methods that attempt to elucidate the origins of dissolved sulfate.

Scientists have also utilized natural variations in isotope measurements that reflect natural and chemical and physical processing to understand how sulfur cycles within ecosystems.[17] More studies have used isotopic distinctions to generate expected values from sulfates sourced from, of most recent interest, biological and anthropogenic activity.[18,19] Specifically, the water isotopes ($\delta^{18}O$) of rain record local meteoric water and other oxidants, while the $\Delta^{17}O$ and $\delta^{34}S$ of sulfate have the potential to uncover more oxidative pathways. Still, such values of some oxides like organic peroxides and nitrogen dioxide remain uncertain.[20] Prior to conducting isotopic studies, baseline data on analyte concentrations and interfering species are required.

1.4 Overview. The research presented herein uses solute concentrations to illuminate sources of sulfur in Houston's rainfall. Along with data from the NADP at a less urban area 60 miles to the west, the data suggests the presence of sea salt aerosol in the precipitation of both areas. However, sea salt aerosols cannot explain total sulfate concentrations, implying the presence of anthropogenic and/or biogenic aerosols. Slightly higher amounts of excess sulfate in the urban site point to predominantly anthropogenic sources, but additional data are required to confirm this hypothesis.

2. Methods

2.1 Sample Preparation. Rain samples were collected on the roof of Keith-Wiess Geological Laboratories at Rice University located at (29.7195° N, -95.4024° W). A passive rain collector with a funnel of diameter 15 cm was situated at the appropriate distance from any obstruction, such as trees, that may result in skewed data.[21] The samples reflect bulk deposition that were collected after single storm events to give representative rain samples. The amount of rain for the first few samples were measured using readings on a graduated syringe. Gravimetric measurements were collected by weighing all samples after October 30th on a lab-grade scale for greater precision. Rainfall depth (mm) was calculated from rainfall volume from the cross sectional area of the collector (π*r^2):

$$\text{depth} = 10 * V / (\pi * r^2),$$

Where V is the volume of rain sample (mL), r is the radius of the rain collector funnel (7.5 cm), and π is the unitless constant of 3.1415.

Samples for the measurement of water isotope ratios were transferred immediately to glass exetainer vials after collection to prevent fractionation by evaporation. Then, a Thermo Orion ROSS Ultra Low Maintenance pH Triode, calibrated using standards of pH 4 and 7, was used to measure 2 mL of sample to determine pH. Low volume samples were all measured for pH, but may have incomplete ion and isotope data. A 60 mL syringe was washed with 30 mL of sample before rinsing a 0.22 micron nitrocellulose mixed ester (MCE) filter with 10 mL of sample and washing each sample container three times. Samples were separated into polypropylene (PP) vials for cation analysis and high-density polyethylene (HDPE) bottles for anion measurements. Cation splits were acidified to a pH of around 2 via the addition of concentrated nitric acid.

2.2 Instruments. Samples were analyzed for anion concentrations using ion chromatography, which yielded the concentrations of Cl^-, NO_3^-, and SO_4^{2-}. Cation concentrations (Na^+, Mg^{2+}, and Ca^{2+}) were measured on an inductively coupled plasma mass spectrometer (ICP-MS). Water isotope data was gathered using cavity ring-down spectroscopy (CRDS). All methods and measurements were conducted at the Department of Earth, Environmental, and Planetary Sciences at Rice University.

2.3 Auxiliary Methods. Information from outside sources was utilized to establish the context of the collected data. Hourly wind data from NOAA was used to assign a weighted average to the period of each rain event.[22] Precipitation data from the National Atmospheric Deposition Program's site at the Attwater Prairie Chicken National Wildlife Refuge (29.6614° N, -96.2594° W), operated by the US Fish and WIldlife Service and the US Geological Survey. Weekly data

from 2019 to 2023 was used to offer longer-term concentration and pH data to complement the collected project samples that span only eight months.[9]

3. Results

3.1 Houston Solutes. The following figures present the concentrations of chloride, nitrate, and sulfate anions in the collected rainwater. The concentration of chloride ranged from 0.33 to 15 ppm, the concentration of nitrate ranged from 0.60 to 14 ppm, and the concentration of sulfate ranged from 0.45 to 13 ppm with means of 3.4, 3.0, and 2.8 ppm respectively. In Figure 3a, all three anions decrease in concentration as the depth of the rainfall increases, indicating the presence of the dilution effect in the rain processing around Houston. The anion concentrations appear to have no definable seasonal variation (Figure 3b). Winds from the south correlate with greater concentrations of all anions; however, distinct relationships are unclear (Figure 3c).

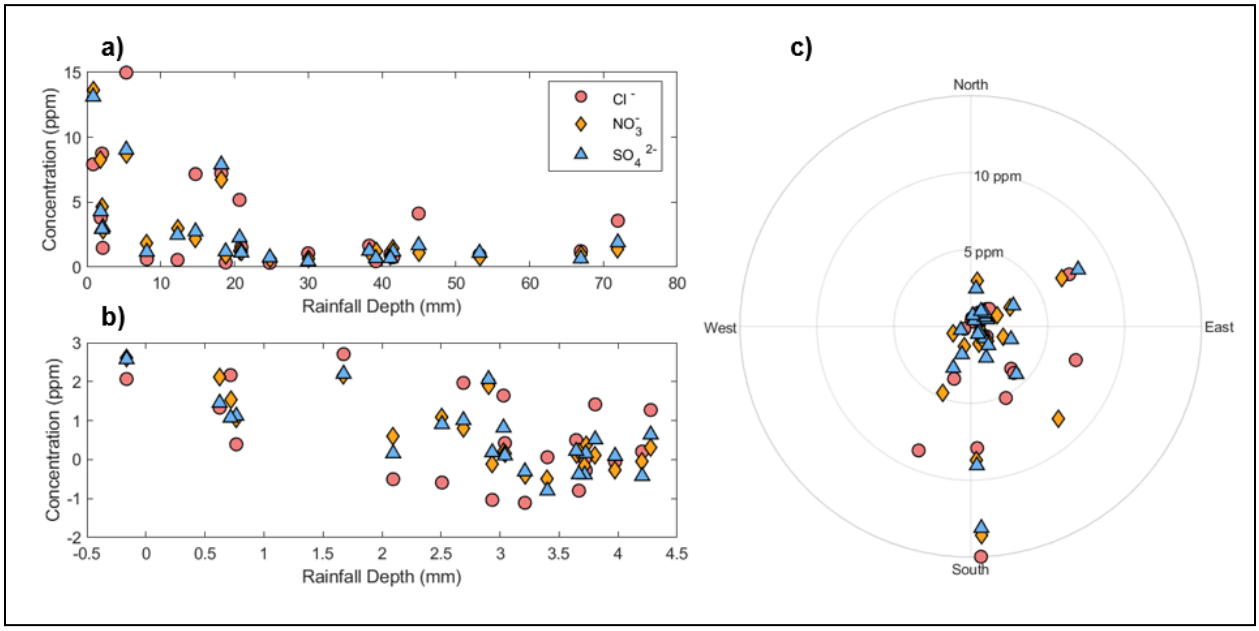

Figure 3: Anion concentrations of KWGL rain samples in relation to **a)** rainfall depth, **b)** across time, and **c)** wind direction.

Cations exhibit similarities to the characteristics of rain anions. The concentration of sodium ranged from 0.0092 to 0.18 mM, the concentration of magnesium ranged from 0.00083 to 0.020 mM, and the concentration of calcium ranged from 0.0064 to 0.038 mM with averages of 0.056, 0.0065, and 0.019 mM. All three cations decrease in concentration as the depth of the rainfall increases, as shown in Figure 4a. The cation concentrations appear to have no definable relationship with seasonality (Figure 4b). The direction of wind flow at the time of precipitation relates to concentration of cations (Figure 4c). Winds from the south and southeast contain 2-3.5 times the concentration of other samples. Similarly, magnesium and calcium concentrations are greater in the rain from the southeast.

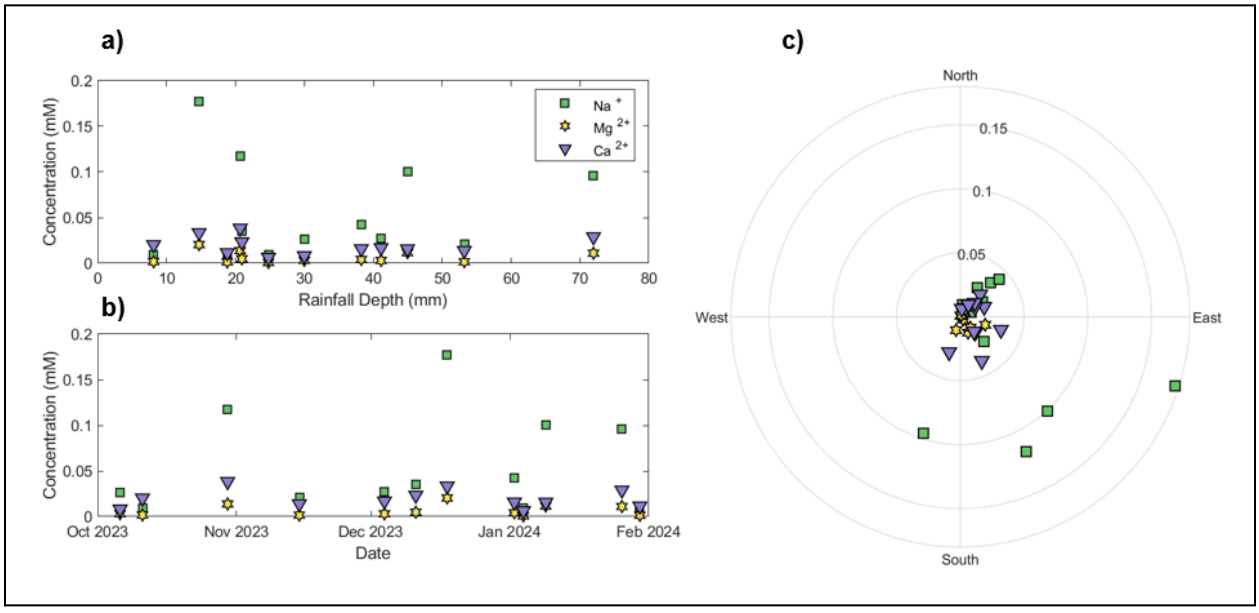

Figure 4: KWGL cation concentrations versus **a)** rainfall depth, **b)** across time, and **c)** wind direction.

As depicted in Figure 5, relationships between anions and cations present a general positive correlation. The strongest direct correlations for KWGL samples are between chloride and sodium with an R^2 value of 0.993 as well as chloride and magnesium with an R^2 of 0.992

(Figure 5a-b). Sulfate and nitrate exhibit weaker positive correlations across all cations, but nitrate has the most scattered data. While sodium's relationship with sulfate suggests a power law, calcium and magnesium exhibit steep, linear slopes. Sodium to chloride molar ratios average at 0.87, around the 0.86 ratio of seawater, but range from 0.54 to 1.02 (Figure 6a). Calcium to sulfate ratios increase with increasing pH which ranges from 6.1 to 7.0, while seawater lies at 0.37 (Figure 6b).

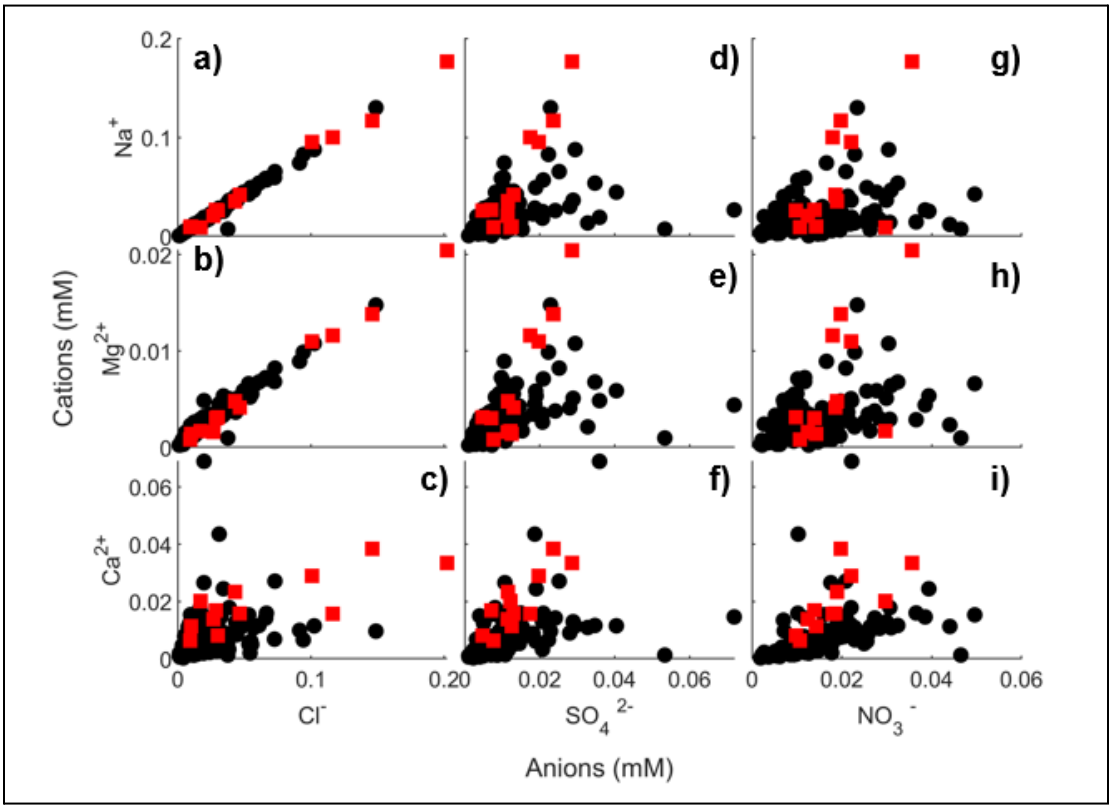

Figure 5: KWGL (red squares) and NADP (black circles) solute molar relationships.

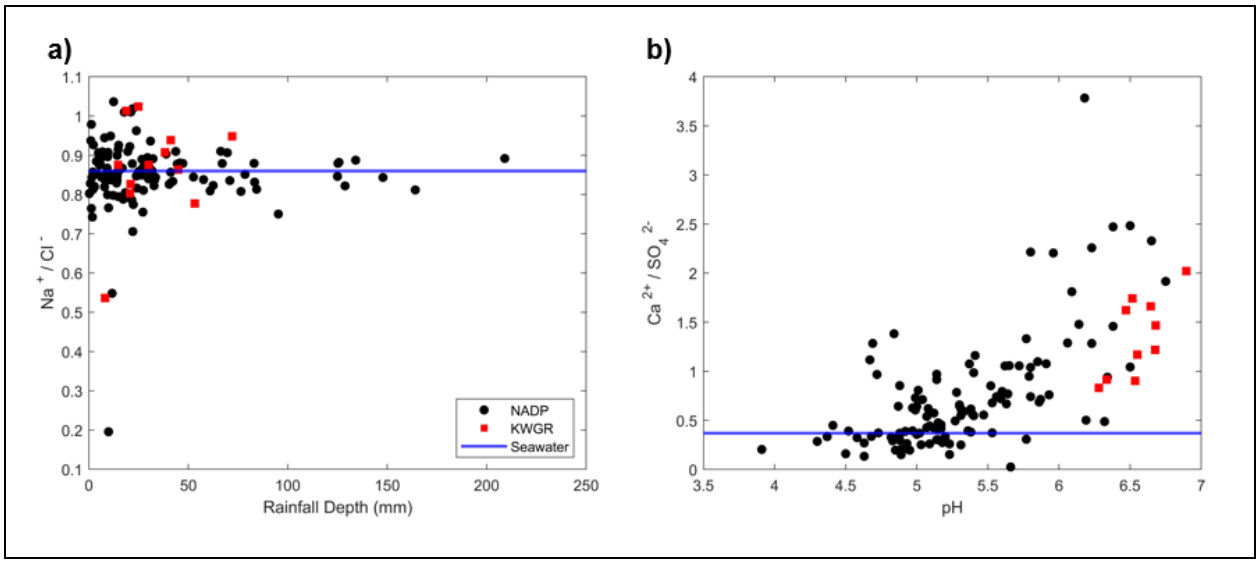

Figure 6: **a)** Na^+:Cl^- molar ratio versus rainfall depth and **b)** Ca^{2+}:SO_4^{2-} molar ratio versus pH as compared to seawater.

Non-sea salt sulfate (nss SO_4^{2-}) of each sample was calculated using the 0.14 molar ratio of seawater sulfate to chloride as follows[23]:

$$\text{nss } SO_4^{2-} = SO_4^{2-}{}_{\text{measured}} - (0.14 \times Cl^-{}_{\text{measured}})$$

where all values are in ppm and assuming that all Cl^- comes from seawater. 58 to 97% of SO_4 in these samples may be attributed to non-sea salt sources under this assumption, with a maximum concentration of 12 and a minimum concentration of 0.30 ppm. Similar to that of the previous ion concentrations, the concentration of non-sea salt sulfate decreases with increasing rainfall depth, and there does not appear to be a well-established relationship over the period of collection (Figure 7a-b). Wind direction does not indicate a relationship with nss SO_4^{2-}, with outliers tending toward samples collected from southeastern winds (Figure 7c). Due to the linear relationship between sulfate and non-sea salt sulfate, greater cation concentrations also correlate with higher amounts of non-sea salt sulfate.

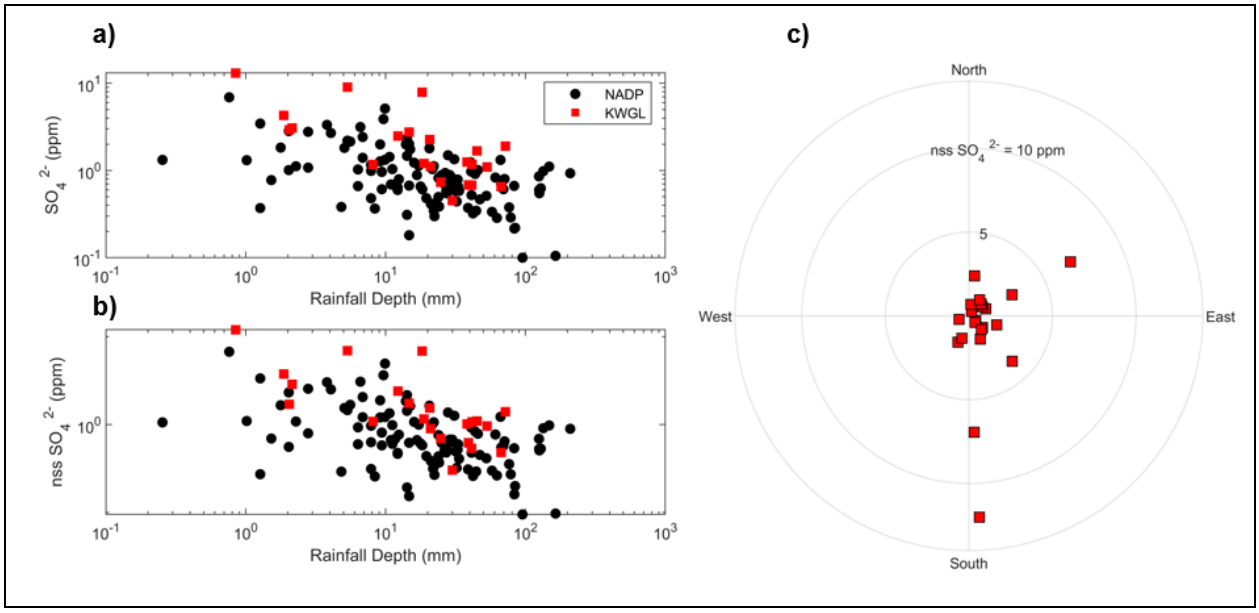

Figure 7: **a)** Total SO_4^{2-} and **b)** nss SO_4^{2-} concentrations of the two collection sites versus depth. **c)** Houston nss SO_4^{2-} with wind direction.

3.2 NADP Solutes. Ion measurements recorded from the NADP exhibit similar relationships as the Houston samples. Chloride concentrations had a maximum of 5.28, a minimum of 0.037, and a mean of 0.92 ppm. Nitrate concentrations ranged from 0.12 to 3.1 with a mean of 0.93 ppm, while sulfate measured between 0.10 and 6.9 with a mean of 1.1 ppm. Concentration of both cations and anions decrease with increasing rain depth (Figure 8). Sodium concentrations had a maximum of 0.13, a minimum of 0.00070, and a mean of 0.022 mM. Magnesium concentrations ranged from 0.00020 to 0.015 with a mean of 0.0030 ppm, while calcium measured between 0.00030 and 0.069 with a mean of 0.0076 ppm.

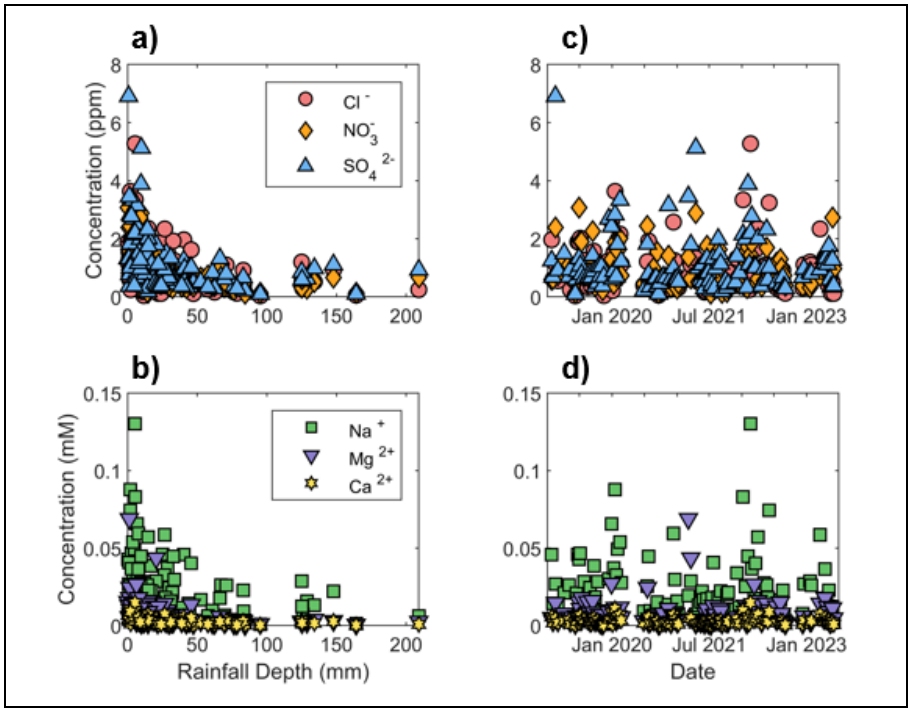

Figure 8: Anion **(a,c)** and cation **(b,d)** concentrations of NADP samples versus rainfall depth and time (2019-2023).

NADP anions and cations exhibit the same positive correlation as the Houston samples (Figure 3), with the strongest relationship also being between chloride and sodium as well as magnesium, with R^2 values of 0.983 and 0.942 (Figure 5). Sodium to chloride molar ratios average around 0.85, but range from 0.20 to 1.0 (Figure 6a), and pH ranges from 3.9 to 6.8 (Figure 6b). Non-sea salt sulfate calculated from NADP data ranged from 0.095 to 6.7 with a mean of 0.98 ppm, with 55 to 99% of total SO_4^{2-} (Figure 7).

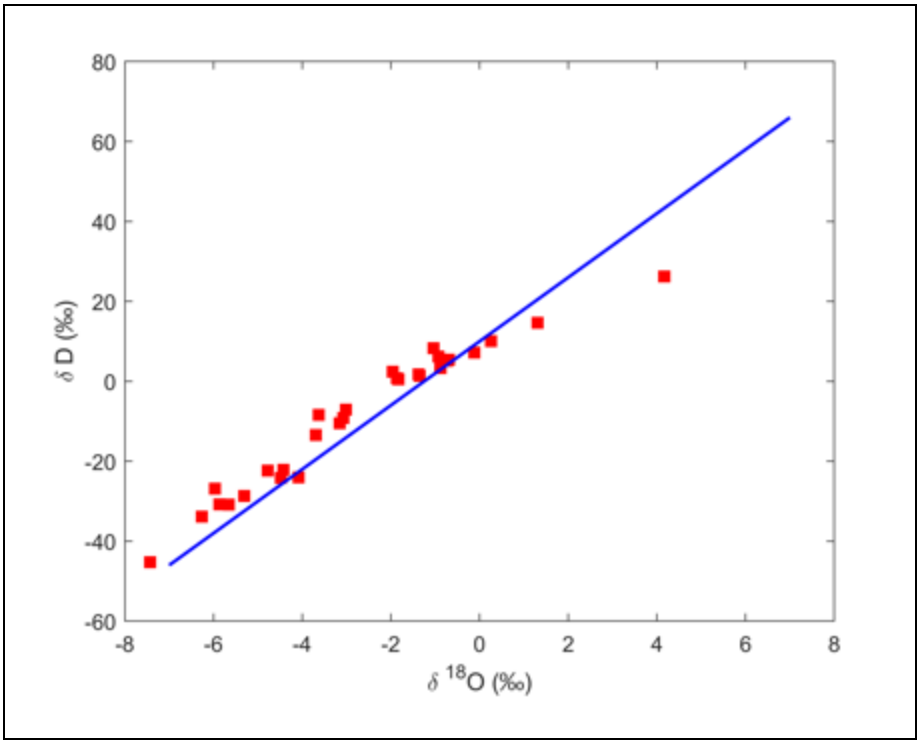

Figure 9: The relationship between **δ**D and **δ**^{18}O of KWGL samples (red squares) with respect to the global meteoric water line (blue).

3.3 Water Isotopes. Figure 9 compares the expected positive correlation of **δ**D and **δ**^{18}O based on the global meteoric water line (MWL) to the measured precipitation samples.[23,24] **δ**D and **δ**^{18}O measurements ranged from -45 to 16‰ and -22 to 5.4‰ respectively. Most measurements lay above the meteoric water line, while 4 samples plot below. The relative departure of deuterium from the MWL trend, called deuterium excess (d-xs), is calculated using the equation below.[24,25,26]

$$\text{d-xs} = \delta D - 8 \times \delta^{18}O$$

While d-xs ranged from 8.01 to 20.9‰, the majority of samples fell above the MWL value of 10‰. Thus, most samples contain more deuterium than expected based on the MWL and weakly decrease in **δ**D as rainfall depth increases. Deuterium excess is inversely related to sulfate

concentration, but does not appear to show any relationship to the wind direction during the rain event (Figure 10).

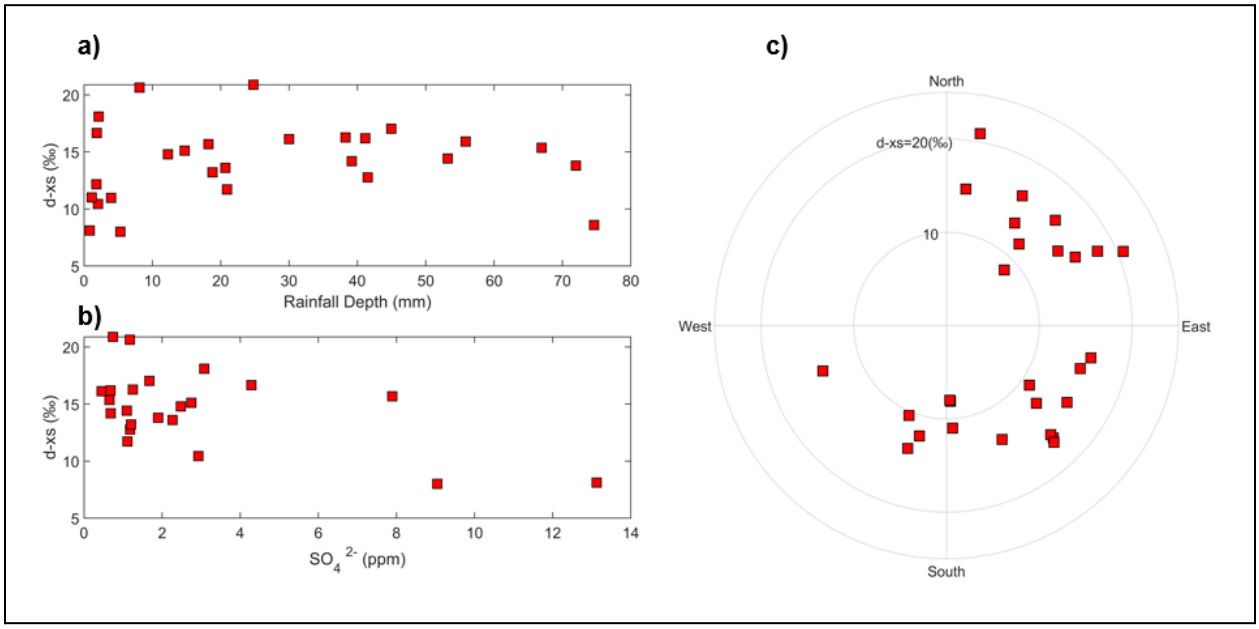

Figure 10: Deuterium excess according to **a)** depth, **b)** total SO_4^{2-}, and **c)** wind direction.

4. Discussion

4.1 Sample Evaporation. Water isotopic data implies that four samples evaporated before measurement, which likely happened during rain collection (Figure 9). Samples that fall below the local meteoric water line had low volumes, suggesting that the rain collector's inlet may not have been fully submerged over the collection period. The evaporated, low-volume samples contain higher concentration of ions than the majority of the data, further establishing the dilution effect. While these samples represent outliers in concentration data, analyzing concentrations with respect to rainfall depth essentially normalizes data to discrepancies in volume. Evaporation also modifies deuterium excess values as seen in Figure 10, a relationship explored in Gat et al.[27]

4.2 Sea Salt. The data shown in Figure 5 explores the relationships of solute concentrations. Most notably, there is a consistent linear relationship between chloride with both sodium and magnesium concentrations for all samples. This correlation points toward the presence of sea salt spray aerosols in the rain collected at both sites. This finding is further corroborated by sodium to chloride ratios. Sea water has a characteristic Na^+ : Cl^- molar ratio of 0.86, which is similar to the 0.85 and 0.87 ratios calculated for the NADP and KWGL samples, respectively (Figure 6a).[28] The nearly constant ratio provides confidence in the aforementioned calculation of nss SO_4^{2-} that assumes all chloride comes from the ocean. Together, these data points record the contribution of sea salt aerosols to rain solutes near the American Gulf Coast.

Overall, KWGL samples contained more total sulfate, normalized by volume, than did those measured by the NADP (Figure 7a). This relationship is further reflected in nss sulfate data (Figure 7b), of which KWGL samples in Houston present higher concentrations than the NADP measurements, confirming that more urban areas should have higher concentrations of total and nss sulfate than neighboring and less industrial locations. The presence of the petrochemical industry around Houston may explain the discrepancy in sulfate concentrations between the measurement sites.

4.3 pH Discrepancy. pH values of the Houston samples fell above that of average rain, calculated to be 5.6.[29] The relationship between Ca^{2+}:SO_4^{2-} molar ratios and rainfall depth confirms that calcium plays a role in determining the pH of rain (Figure 6b).[30,31] Calcium-bearing phases like carbonate minerals can increase the buffering capacity of rain because they they readily react with strong acids. Winds carrying calcium carbonate mineral dust transported from nearby mining operations or arid stretches of land (e.g. Permian Basin) could be a contributor; however,

this project has not collected enough data to determine dust sources. Given the locations of each site, it is reasonable that NADP samples have greater concentrations of calcium ions due to its proximity to arid regions. The greater Houston area houses concrete production facilities, which repurposes fly ash, typically from coal-fired power plants, containing calcium oxide (CaO).[32] Such fly ash may also explain the high concentrations of calcium that affect atmospheric composition and subsequent precipitation.

5. Conclusion

5.1 Summary. The data presented here showcase a first step toward deciphering the sources of sulfate in Hosuton's rainfall. Measurements collected at Rice University show greater concentrations than an NADP site about 60 miles west on a wildlife reserve. Both regions present relationships similar to that of sea salt, suggesting the influence of sea spray aerosols on sulfate concentration in coastal rain. Of greater significance is the finding that not all sulfate can be attributed to sea salt, but instead there is a signal of non-sea salt sulfate at the ppm level in both samples. Water isotopes did not exhibit a correlation with non-sea salt sulfate; as such, further research is needed to elucidate the sources of this sulfate as discussed in the following section. pH measurements encapsulate the complexities of rainfall interactions, yet point toward the effect of mineral dust in buffering the acidity of Houston-area precipitation which mitigates one of the known negative consequences of excess SO_4^{2-}.

5.2 Next Steps. Beyond the analysis of ions, a more robust method for determining aerosol sources uses isotopic ratios of sulfur and oxygen as signals of specific sources, and can even be used to suggest the particle's pre-processing steps. Previous literature has used sulfur isotope

data in order to differentiate sources of sulfate in rainfall. This data is invaluable in this work due to its ability to capture fractionation of sulfur compounds depending on its origins. Standard methods like isotope ratio mass spectroscopy (IRMS) use around 50 mg of analyte for sulfur and oxygen isotope measurements, which would require on the order of hundreds of mL of rainwater because it is so dilute. This presents a skew in data as these signals can only be measured during big storm events, leaving the more frequent low volume samples under-analyzed. For this reason, it is important to investigate how new, cutting-edge instruments can be leveraged to improve investigations of the sources of sulfur in rainwater. Future work will be focused on calibrating a new electrospray quadrupole Orbitrap mass spectrometer (ESMS) with a conventional IRMS for use in oxygen and sulfur isotope measurements.[32] This will greatly improve sulfur dioxide tracing because ESMS requires roughly 1000 times less sulfate compared to the traditional IRMS methods.

Table 1: Sulfur isotopic data for in-house sulfate standards using IRMS.

Sample	**SO_4^{2-} Concentration (ppm)**	**^{34}S (‰)**
Sodium sulfate (lab grade)	1300	-5.3
White Sands (gypsum)	360	12.1
Moekoepi formation (gypsum)	660	-17.5
Central Texas Mine (gypsum)	1400	15.1
Palo Duro (gypsum)	850	9.7
Hanksite crystal	1000	13.8

Current methods to prepare the rain samples for analysis using IRMS have been tested on six sulfate solutions made from lab grade sodium sulfate, hanksite, and four field samples of gypsum. The above solutions have also been prepared and tested for sulfur isotopes on the lab's

new ESMS to operate as in-house standards because there is no widely accepted sulfate standard for these measurements. Preliminary measurements indicate that both methods yield the same results.

6. References

(1) Overview of Sulfur Dioxide (SO2) Air Quality in the United States. Environmental Protection Agency. https://www.epa.gov/system/files/documents/2022-08/SO2_2021.pdf

(2) Heal, M. R.; Kumar, P.; Harrison, R. M. Particles, Air Quality, Policy and Health. Chem. Soc. Rev. 2012, 41 (19), 6606–6630. https://doi.org/10.1039/C2CS35076A.

(3) Cofala, J.; Amann, M.; Heyes, C.; Wagner, F.; Klimont, Z.; Posch, M.; Schöpp, W.; Tarasson, L.; Jonson, J. E.; Whall, C.; Stavrakaki, A. Analysis of Policy Measures to Reduce Ship Emissions in the Context of the Revision of the National Emissions Ceilings Directive.

(4) Cooley, S.; Schoeman, D.; Bopp, L.; Boyd, P.; Donner, S.; Ito, S.-I.; Kiessling, W.; Martinetto, P.; Ojea, E.; Racault, M.-F.; Rost, B.; Skern-Mauritzen, M.; Ghebrehiwet, D. Y. Ocean and Coastal Ecosystems and Their Services. In Climate Change 2022: Impacts, Adaptation and Vulnerability. Contribution of Working Group II to the Sixth Assessment Report of the Intergovernmental Panel on Climate Change; Pörtner, H.-O., Roberts, D. C., Tignor, M. M. B., Poloczanska, E. S., Mintenbeck, K., Alegría, A., Craig, M., Langsdorf, S., Löschke, S., Möller, V., Okem, A., Rama, B., Eds.; Cambridge University Press, 2022.

(5) Chen, J.; Zhang, H.; Liu, L.; Zhang, J.; Cooper, M.; Mortimer, R. J. G.; Pan, G. Effects of Elevated Sulfate in Eutrophic Waters on the Internal Phosphate Release under Oxic Conditions across the Sediment-Water Interface. Science of The Total Environment 2021, 790, 148010. https://doi.org/10.1016/j.scitotenv.2021.148010.

(6) Stallard, R. F. Atmospheric Inputs to Watersheds of the Luquillo Mountains in Eastern Puerto Rico.

(7) Intergovernmental Panel On Climate Change. Climate Change 2021 – The Physical Science Basis: Working Group I Contribution to the Sixth Assessment Report of the Intergovernmental Panel on Climate Change, 1st ed.; Cambridge University Press, 2023. https://doi.org/10.1017/9781009157896.

(8) Smith, S. J.; Andres, R.; Conception, E.; Lurz, J. Historical Sulfur Dioxide Emissions 1850-2000: Methods and Results; PNNL-14537, 15020102; 2004; p PNNL-14537, 15020102. https://doi.org/10.2172/15020102.

(9) National Atmospheric Deposition Program (NRSP-3). 2022. NADP Program Office, Wisconsin State Laboratory of Hygiene, 465 Henry Mall, Madison, WI 53706.

(10) Parungo, F.; Nagamoto, C.; Hoyt, S.; Humberto Bravo, A. The Investigation of Air Quality and Acid Rain over the Gulf of Mexico. Atmospheric Environment. Part A. General Topics 1990, 24 (1), 109–123. https://doi.org/10.1016/0960-1686(90)90446-T.

(11) Aneja, V. P.; Aneja, A. P.; Adams, D. F. Biogenic Sulfur Compounds and the Global Sulfur Cycle. Journal of the Air Pollution Control Association 1982, 32 (8), 803–807. https://doi.org/10.1080/00022470.1982.10465466.

(12) Finlayson-Pitts, B. J.; Jr, J. N. P. Chemistry of the Upper and Lower Atmosphere: Theory, Experiments, and Applications; Elsevier, 1999.

(13) Liu, T.; Chan, A. W. H.; Abbatt, J. P. D. Multiphase Oxidation of Sulfur Dioxide in Aerosol Particles: Implications for Sulfate Formation in Polluted Environments. Environ. Sci. Technol. 2021, 55 (8), 4227–4242. https://doi.org/10.1021/acs.est.0c06496.

(14) Ervens, B. Modeling the Processing of Aerosol and Trace Gases in Clouds and Fogs. Chem. Rev. 2015, 115 (10), 4157–4198. https://doi.org/10.1021/cr5005887.

(15) Brandt, C.; van Eldik, R. Transition Metal-Catalyzed Oxidation of Sulfur(IV) Oxides. Atmospheric-Relevant Processes and Mechanisms. Chem. Rev. 1995, 95 (1), 119–190. https://doi.org/10.1021/cr00033a006.

(16) Liang, J.; Jacobson, M. Z. A Study of Sulfur Dioxide Oxidation Pathways over a Range of Liquid Water Contents, pH Values, and Temperatures. Journal of Geophysical Research: Atmospheres 1999, 104 (D11), 13749–13769. https://doi.org/10.1029/1999JD900097.

(17) Fuller, R. D.; Mitchell, M. J.; Krouse, H. R.; Wyskowski, B. J.; Driscoll, C. T. Stable Sulfur Isotope Ratios as a Tool for Interpreting Ecosystem Sulfur Dynamics. Water Air Soil Pollut 1986, 28 (1), 163–171. https://doi.org/10.1007/BF00184078.

(18) Nriagu, J. O.; Holdway, D. A.; Coker, R. D. Biogenic Sulfur and the Acidity of Rainfall in Remote Areas of Canada. Science 1987, 237 (4819), 1189–1192. https://doi.org/10.1126/science.237.4819.1189.

(19) Zheng, M.; Song, D.; Zhang, D.; Zhao, Z. Variability of Sulfur and Oxygen Isotope Values within Wet Precipitation and Its Correlation with Diminished Anthropogenic Sulfur Dioxide (SO2) Emission. Atmospheric Environment 2024, 317, 120185. https://doi.org/10.1016/j.atmosenv.2023.120185.

(20) Jenkins, K. A.; Bao, H. Multiple Oxygen and Sulfur Isotope Compositions of Atmospheric Sulfate in Baton Rouge, LA, USA. Atmospheric Environment 2006, 40 (24), 4528–4537. https://doi.org/10.1016/j.atmosenv.2006.04.010.

(21) The Global Network of Isotopes in Precipitation (GNIP) team. IAEA/GNIP precipitation sampling guide. https://www.iaea.org/services/networks/gnip.

(22) Midwestern Regional Climate Center's Application Tools Environment (cliMATE). 2023. Midwestern Regional Climate Center. 915 West State Street, West Lafayette, IN 47907.

(23) Keene, W.C., Pszenny, A.A.P., Galloway, J.N. and Hawley, M.E. Sea-Salt Corrections and Interpretation of Constituent Ratios in Marine Precipitation. Journal of Geophysical Research, 1986, 91, 6647-6658. https://doi.org/10.1029/JD091iD06p06647

(24) Craig, H. Isotopic Variations in Meteoric Waters. Science 1961, 133 (3465), 1702–1703.

(25) Dansgaard, W. Stable Isotopes in Precipitation. Tellus 1964, 16 (4), 436–468. https://doi.org/10.3402/tellusa.v16i4.8993.

(26) Chen, F.; Zhang, M.; A. Argiriou, A.; Wang, S.; Zhou, X.; Liu, X. Deuterium Excess in Precipitation Reveals Water Vapor Source in the Monsoon Margin Sites in Northwest China. Water 2020, 12 (12), 3315. https://doi.org/10.3390/w12123315.

(27) Gat, J.R., Bowser, C.J., Kendall, C. The contribution of evaporation from the Great Lakes to the continental atmosphere: estimate based on stable isotope data. Geophys. Res. Lett. 1994, 21 (7), 557-560. https://doi.org/10.1029/94GL00069.

(28) Han, M.W. "Pilson, Michael E. Q.: An introduction to the chemistry of the sea." CHOICE: Current Reviews for Academic Libraries, vol. 51, no. 1, Sept. 2013, p. 110.

(29) Park, S.-M.; Seo, B.-K.; Lee, G.; Kahng, S.-H.; Jang, Y. W. Chemical Composition of Water Soluble Inorganic Species in Precipitation at Shihwa Basin, Korea. Atmosphere 2015, 6 (6), 732–750. https://doi.org/10.3390/atmos6060732.

(30) Liljestrand, H. M. Average Rainwater pH, Concepts of Atmospheric Acidity, and Buffering in Open Systems. Atmospheric Environment (1967) 1985, 19 (3), 487–499. https://doi.org/10.1016/0004-6981(85)90169-6.

(31) Cooper, Hal B. H., Jose A. Lopez, and Jerry M. Demo. “Chemical Composition of Acid Precipitation in Central Texas.” Water, Air, and Soil Pollution 6, no. 2 (June 1, 1976): 351–59. https://doi.org/10.1007/BF00182876.

(32) Estakhri, C. K.; Saylak, D. Reducing Greenhouse Gas Emissions in Texas with High-Volume Fly Ash Concrete. Transportation Research Record, 1941.

(33) Neubauer, C.; Crémière, A.; Wang, X. T.; Thiagarajan, N.; Sessions, A. L.; Adkins, J. F.; Dalleska, N. F.; Turchyn, A. V.; Clegg, J. A.; Moradian, A.; Sweredoski, M. J.; Garbis, S. D.; Eiler, J. M. Stable Isotope Analysis of Intact Oxyanions Using Electrospray Quadrupole-Orbitrap Mass Spectrometry. Anal. Chem. 2020, 92 (4), 3077–3085. https://doi.org/10.1021/acs.analchem.9b04486.